

Filtering of Cardiac and Power Line in Surface Respiratory EMG Signal

S. Yacoub^{1,2}, K. Raouf³, and H. Eleuch^{1,4}

¹Institut National des Sciences Appliquées et de Technologies INSAT BP676
Tunis Cedex, Tunisie
Email Address: *slimyacoub@insat.rnu.tn*

²Laboratoire des Systèmes et Traitement du Signal LSTS ENIT Tunisie

³Laboratoire des images et des signaux (LIS) ENSIEG, BP46, 38402 St Martin d'Hères, France

⁴The Abdus Salam Centre for Theoretical Physics, ICTP, Strada Costiera 11, 34014 Trieste, Italy

Received July 4, 2008; Revised September 14, 2008

Biomedical *EMG* signal is contaminated by many noise sources as the electrocardiogram *ECG* artefact and the power line interference *PLI* artefact. It's difficult to filter these noises from *EMG* signal, and errors resulting from filtering can alter the signal. In order to solve this problem, we present in this paper an adaptative interference filter with a variable step size parameter for the removal of the two principal noises (*ECG* and *PLI*) which disturb the surface electromyography signal (Diaphragm), the "Adaptive Interference Canceller" (*AIC*) for the *PLI* and the "Cascade Adaptive Canceller" (*CAC*) for the *ECG*. The algorithms proposed require a reference signal that is correlated with the noise contaminating the signal. The noise references are then extracted : first with a noise reference mathematically constructed using two different cosine functions; $50Hz$ (the fundamental) function and $150Hz$ (the first harmonic) function for the power line interference and second with a matching pursuit technique combined to an *LMS* structure for the *ECG* artefact estimation. The proposed procedures require only one channel to both estimating the adaptive filter input reference and the *EMG* signal. The proposed techniques of filtering are evaluated using both computer simulations and real *EMG* records, and its efficiency in interference cancellation is compared to already conducted research.

Keywords: Surface *EMG*, adaptive noise canceller, matching pursuit, *ECG*, power line interference, diaphragm *EMG*.

1 Introduction

The Diaphragm electromyographic signal conveys important information about the respiratory control mechanism [16] especially in the case of long-time monitoring. The ma-

major problem with EMG signal recorded by surface electrode is its bad signal to noise ratio. However the principal artifacts which often disturb *EMG* signal are the electrode noise [12], the electrode motion artefact, the *ECG* artifact [4, 8, 26], and the electromagnetic interference $50Hz$ and its harmonic $150Hz$ [6].

The spectra of *ECG* artifact and EMG signal overlap in some frequency range moreover the variable amplitude ratio between them caused by the non-stationary *EMG* signal nature made the *ECG*, very difficult to eliminate [9]. The second important artifact that contaminates the *EMG* signal concerned the power line interference which can be much larger than the EMG its self. This noise arises from the power lines and the electric equipment. The frequency of these fields is at the frequency of the alternative current power supply ($50Hz$) and its harmonics. In order to reduce the magnitude of this artefact, first of all, we tried to realize a good preparation of the body skin indeed the skin is abraded and cleaned with abrasive cream and alcohol. Second to reduce the effect of the cable length the signals are differentially amplified [14, 23] twice. However, these changes may not always be sufficient in case of a deep contaminated surrounding and weak muscular activities and it will be necessary to reduce the interference using other means. The use of analogical or digital filters of fixed band centered on $[20 - 40Hz]$ for the *ECG* signal (maximum energy of *ECG*) and on $50Hz$ and on $150Hz$ for the power line interference *PLI* fails. Indeed these filters allowed the reduction of the noises they also eliminate some useful signal components. A solution to this problem is proposed by applying , the LMS adaptive algorithm [27, 28] but without introducing supplementary electrodes to the noise reference in order to minimize the presence of electronics.

2 Experimental Configuration

We apply in our analysis bipolar technique. The pair of electrodes is situated on 7th and 8th intercostals spaces and at two centimetres of junction chondrocostal on the left of the sternum. This exactly specific location has been chosen in order to particularly pay attention to diaphragmatic EMG in his costal part. We first note that we must use the reference electrode, which is situated on the wrist of the patient. In fact, the two electrodes are connected to a differential amplifier of instrumentation. We use three millimetre diameter metallic electrodes. The distance between the electrodes of one pair is fixed at 36 millimetres and it is imposed by the distance between two intercostals spaces. The electrodes are carefully positioned and situated on clean skin, which is beforehand abraded and cleaned with abrasive cream and alcohol. The signals are differentially amplified at twice. The first level amplifies by using the instrumentation amplifier (INA101). As soon as the second level amplifies (LF442), it filters frequency band $[10 - 230Hz]$ [11]. Then, it digitizes at $1024Hz$ sampling frequency (one channel 12 bits ADC and are processed by digital signal processor Analog device ADC 2105). The recordings are obtained from subjects, who are

stretched out. The obtained recordings have a cardiac rhythm turning around to 60 at 90 and having a quiet respiratory cadence breaths. The analysis selected window is chosen equal to 8192 samples (8 seconds).

3 Alternating Current Power Line Interference Filtering

The electromagnetic components $50Hz$ and harmonics $150Hz$ overlap the respiratory surface EMG signal, as well as frequency and time. The classical filtering methods using a moving average window [15,17] or a narrow band rejector filter centered at the fundamental frequency [10] filtered simultaneously both the electromagnetic noise and the useful *EMG* components. These approach may be an acceptable compromise if only a rough EMG amplitude estimate is of interest. So, they are not really adaptable to our case study. However Barata [2], estimates the amplitude and phase of the power line interference signal from a clean *EMG* recording segment, then a signal with the same amplitude and phase was generated and subtracted from the whole length of the noisy signal. This method will fail if the amplitude and phase change during the *EMG* recording session. Other techniques use the adaptable filters type LMS (Least Mean Square) which were suggested in [1, 3, 27]. These techniques might give interesting results especially according to *ECG* recording signal case. These methods can be applied for interference rejection if a reference noise can be obtained simultaneously with the corrupted signal. Then the reference input is adaptively filtered and subtracted from the original noisy signal. Widrow suggests a reference input constructed with a fixed delay Δ inserted in the reference input drawn directly from the primary input. The delay chosen must have a sufficient length to cause the respiratory *EMG* signal components in the reference input decorrelated from those in the primary input. The interference components will remain correlated with each other because of their periodic nature. The evaluation of the autocorrelation function of a respiratory *EMG* signal shows that the delay must have a sufficient length 150 milliseconds [29]. To enhance the signal to noise ratio (*SNR*) Bahoura proposes in [1] the same *LMS* structure but estimates the reference noise signal with a band-pass filter centered on the electromagnetic interference. However, it is not really sufficient because of the presence of useful signal *EMG* in electromagnetic components.

3.1 The algorithm

In this section, we have compared the performances by applying two combined adaptive techniques. The two methods for respiratory *EMG* estimation require an estimation of power line interference *PLI* as a reference signal \widehat{PLI}_{ref} so that an LMS adaptive filter can be used to cancel *PLI* in the contaminated *EMG* signal.

The first combined adaptive technique (*AIC*) follows two steps. The first step consists

in generating an input reference $\widehat{PLI}_{ref} = \cos(\omega_{50}t) + \cos(\omega_{150}t)$ made of a pure cosine functions mathematically constructed; $50Hz$ (the fundamental) function and $150Hz$ (the first harmonic) function. However, in the second step the the output of the filter \widehat{PLI} is estimated to match the noise PLI in the primary input (adaptive filter type LMS) and subtracted from it to obtain the EMG estimated signal (see Fig.3. 1). The filter is optimal by minimizing the least mean square error ε_j (equation 3.1) [27, 28].

The second combined adaptive technique(B_F) follows also two steps: the first step applies pass-band filter centered at the fundamental frequency $50Hz$ ($[49.5 - 50.5Hz]$) and its harmonics $150Hz$ ($[149.5 - 150.5Hz]$) in order to extract the PLI noise reference signal. The second step applies again the same processing shown in the first adaptive technique (AIC).

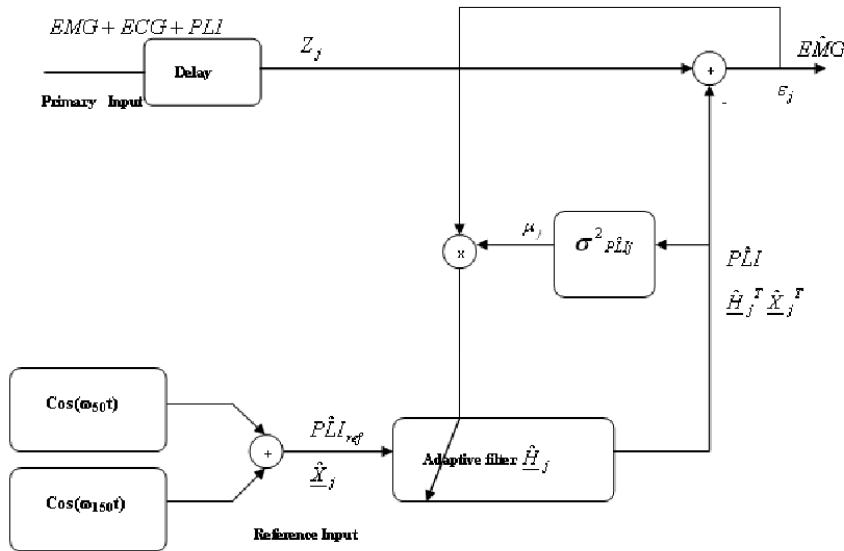


Figure 3.1: The (AIC) structure of adaptive power line interference filtering : $z_j = EMG + ECG + PLI$, raw signal; EMG , signal of interest ; PLI , noise; \widehat{PLI}_{ref} , reference noise ; \widehat{PLI} , estimate of the noise with the adaptive filter ; \widehat{H}_j , adaptive filter coefficient ; \widehat{EMG} , filtered signal.

The coefficients \widehat{H}_{j+1} of the adaptive filter are computed according to equation (3.2). The error ε_j represents the difference between the original signal Z_j and the adaptive filter output $\widehat{H}_j^T X_j^T (\widehat{PLI})$.

The reference input \widehat{PLI}_{ref} is the sum of two cosinusoidal signals with respectively $50Hz$ and $150Hz$ frequencies and zero phases.

The fundamental equations of this algorithm are:

$$\varepsilon_j = Z_j - \hat{H}_j^T \underline{X}_j^T, \quad (3.1)$$

where \hat{H}_j is the reference input \widehat{PLI}_{ref} , and \hat{H}_j is the adaptive filter coefficients.

$$\hat{H}_{j+1} = \hat{H}_j + 2\mu\varepsilon_j \hat{X}_j, \quad (3.2)$$

$$j : 1 \longrightarrow M, \quad (3.3)$$

$$\mu_{j+1} = \mu_j + \sigma_{\widehat{PLI}_j}^2 + \frac{1}{1 + \sigma_{\widehat{PLI}_j}^2}, \quad (3.4)$$

Z_j is the original signal ($EMG + ECG + PLI$), ε_j is the estimated EMG signal with LMS algorithm and μ is the Rate of convergence and accuracy of the adaptation process.

The noise PLI of the primary input and the reference signal \widehat{PLI}_{ref} are assumed to be correlated.

The finite impulse response of the adaptive filter \hat{H}_j is carried out with M coefficients.

$\sigma_{\widehat{PLI}_j}^2$ is the power of the noise estimation \widehat{PLI} .

M should be sufficiently long in order to compensate the phase shift that may exists between the synthesized \widehat{PLI}_{ref} signal and the PLI of the raw respiratory EMG signal.

A sufficient length of an LMS filter using the adaptive filter structure can be formulated in the following expression

$$M > \frac{fs}{fpli}, \quad (3.5)$$

where fs is the sampling frequency and $fpli$ is the lowest interference frequency

3.2 Results

3.2.1 Performance indicators

To compare different methods of power line interference filtering, the Total Power in percent ($TP\%$) is calculated according to

$$TP_i\% = 100 \frac{\sum_{i=f_1}^{f_2} (P_s(i))^2}{\sum_{i=f_1}^{f_2} (P_r(i))^2}, \quad (3.6)$$

where $P_s(i)$ and $P_r(i)$ are respectively the spectral densities amplitudes of the processed signal and the raw EMG signal contaminated with obvious ECG artefacts and power line interference artefacts PLI per frequency bins. f_i are frequency bins.

To evaluate the effect of the processed methods on the PLI and respiratory EMG signal separately we use the EMG specific segments ($TP_{EMG}\%$) free of PLI and PLI specific segments ($TP_{PLI}\%$) free of EMG .

3.2.2 Performance evaluation

We present in Figure 3.2 computer simulations demonstrating the performance of our adaptive algorithm (*AIC*). So we construct EMG respiratory signal contaminated by pure power line interference *PLI* following two-step procedures. First, cosine functions with $50Hz$ and $150Hz$ frequency are generated and then modulated by a 1 Hz cosine function frequency to produce the simulated *SPLI* signal, as shown in Fig. 3.2(a). Second, a real respiratory EMG signal measured between the 7th and the 8th intercostals space in one subject (Fig. 3.2(b)) is added to the simulated pure *SPLI* as shown in Fig. 3.2(c) to produce the contaminated respiratory EMG signal. The filtered respiratory *EMG* signal, recovered from the proposed algorithm, is shown in Fig. 3.2(d). This figure suggests that the original respiratory EMG features are mostly preserved while suppressing the power line interference Fig. 3.2(e) present the reference noise signal \widehat{PLI}_{ref} .

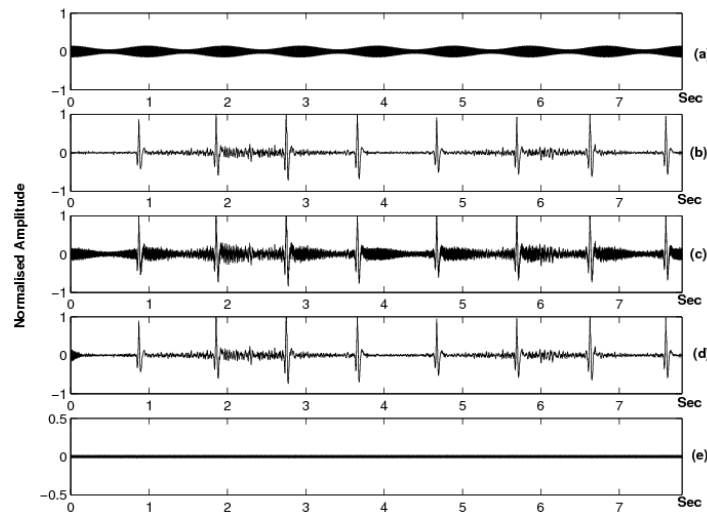


Figure 3.2: Simulation example of power line interference filtering: (a) the simulated *SPLI* signal; (b) real respiratory *EMG* signal measured between the 7th and the 8th intercostals space in one subject; (c) the constructed respiratory *EMG* signal. using (a) and (b) ; (d) the filtered respiratory *EMG* signal; (e) the reference noise signal \widehat{PLI}_{ref} .

The effects of the (*AIC*) cleaning technique are evaluated through different levels of signal-to-noise ratio between respiratory EMG signal and simulated *SPLI* signal (13 4 0 -3 -6 -9 -12db). Table 3.1 demonstrates that this method removes more than 90% of *PLI* across all the SNR level

Total Power in Percent (TP%)	
SNR Level(db) (EMG/PLI)	PLI evaluation
13	96
4	94
0	94
-3	92
-6	92
-9	91
-12	90

Table 3.1: The Total Power (TP%) of a 50 and 150 Hz power line interference extracted from a contaminated respiratory EMG signal relative to a Pure simulated 50 and 150 Hz interference (PLI) in percent, TP mean is evaluated with two segments 49 to 51 Hz range for the 50 Hz and over the 149 and 151 Hz range for the 150Hz for PLI.

3.2.3 Application to real respiratory EMG signal

In this section we will compare the methods which are used to estimate the respiratory EMG signal, described in section 3.1 : two combined techniques: our method (AIC) and behoura adaptive filter ($B.F$) applied to the EMG case. The difference between them involved the reference estimation procedure. Specially, the first method (AIC) estimates the reference by using synthesized cosine functions while the second method ($B.F$) uses for the extraction of the reference a band pass filter varying from 49.5 to 50.5Hz and from 149.5 to 150.5Hz.

In order to prove the efficiency of the suggested method compared to the one designed in [1]. We present in Fig. 3.3a the power spectral density of the raw respiratory EMG signal contaminated with ECG and power line interference signal. Fig 3.3b shows the spectral densities of the adaptive filter output. when the reference is carried out by generating cosines function (Fig.3.3c) (AIC) method. On the contrary Fig 3.3d displays the spectral density of the filtered signal when we apply a band-pass filters ($[49.5 - 50.5Hz]$ and $[149.5 - 150.5Hz]$) ($B.F$) method as a reference noise (Fig 3.3e) It's clear from this Figure that the (AIC) method (Fig.3.3b) reduces considerably the undesirable EMG spectral components around 50Hz and 150 Hz frequency compared to the case of ($B.F$) method as shown in Fig.3.3d.

Respiratory signal contaminated by ECG signal and power line interference signal is shown in Fig. 3.4a. Fig.3.4b and Fig. 3.4c represent respectively the estimation of power line Interference signal \widehat{PLI} and respiratory EMG signal \widehat{EMG} applying the already designed method AIC . Using this proposed method we can note substantial cancellation of the PLI artefact as shown in Figure 3.4.

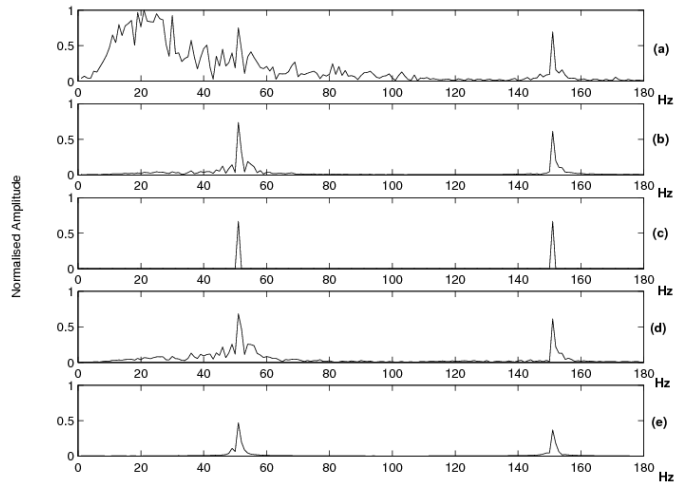


Figure 3.3: Power spectral densities of: (a) raw respiratory *EMG* signal contaminated with *ECG* and Power line interference signal ; (b) filtered signal using (*AIC*) method ; (c) reference noise signal using (*AIC*) method ; (d) filtered signal using (*B-F*) method.; (e) reference noise signal using (*B-F*) method.

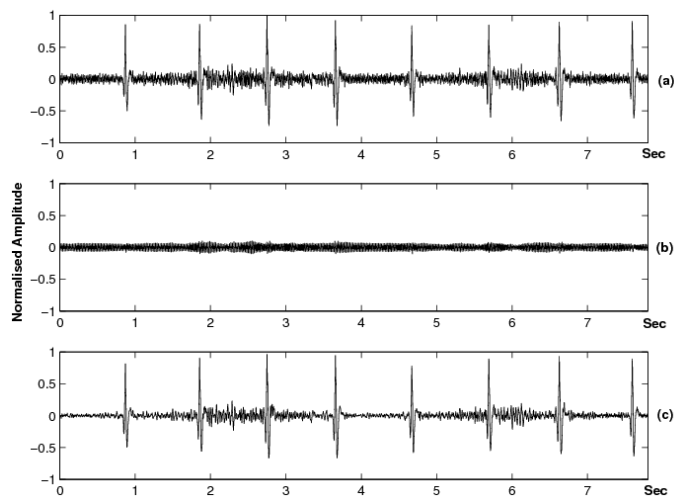


Figure 3.4: Power line interference artifact removal with *AIC* method: (a) Raw surface respiratory *EMG* signal contaminated with *ECG* and power line interference signals; (b) Power line interference estimation; (c) Respiratory *EMG* signal after power line interference subtracting.

Total Power in Percent (TP%)			
	SNR Level(db)(EMG/PLI)	$B.F$ method	AIC method
PLI evaluation	5	90	93.5
$EMG_{distortion}$	5	24	4.9

Table 3.2: The Total Power (TP%) of a 50 and 150 Hz power line interference extracted from a contaminated respiratory EMG signal relative to a Pure simulated 50 and 150 Hz interference (PLI) in percent, TP mean is evaluated with three segments: 1-45Hz, 55-145Hz and 155 -250Hz, for EMG and with two segments 49 to 51 Hz range for the 50 Hz and over the 149 and 151 Hz range for the 150Hz for PLI ($B.F$: Bahoura adaptive filter; AIC : the new proposed method).

To quantify the effects of the proposed methods on the PLI and the EMG spectral content separately, we evaluate the TP of the 50Hz and 150Hz (PLI), over the 49 to 51Hz range for the 50Hz and over the 149 and 151Hz range for the 150Hz. Table 3.2 depicts the Total power mean ($TP\%$) of PLI cleaned signal relative to the PLI contained in the raw signal in percentage, evaluated with the two segments described above. However, The Total Power mean ($TP\%$) of the cleaned respiratory EMG signal, relative to the raw respiratory EMG signal in percentage, is calculated to avoid PLI over the 1 to 45Hz range, the 55 to 145Hz range and the 155 to 250Hz range. We present as well in Table2. the Total power ($TP\%$) mean of respiratory EMG cleaned signal relative to the raw respiratory EMG signal in percentage, evaluated in frequency domain mentioned above. It's clear that the (AIC) method preserves more than 95% of spectral power of EMG features while this method suppresses more than 93.5% electromagnetic interference PLI spectral power. However, we note for ($B.F$) methods more than 24% of power alteration in EMG .

4 Electrocardiogram Artifact Filtering

The major problem with EMG respiratory surface signal is the ECG Electrocardiogram artefact. Various techniques have been proposed to reduce ECG artefact from the EMG. In fact, some of them suggested a non-linear filtering [18] based on a statistical technique. This method requires intensive matrix computation making it inappropriate for real time application. Other method developed a high-pass cut off frequency to estimate the spectral component of the EMG [25], because ECG signal overlaps in frequency domain [13] with the surface respiratory EMG . This method will result in a signal information loss. The adaptive algorithm based on that of Widrow [22, 27, 28] is an effective method to separate an interfering signal from a signal of interest. In this noise canceller the ECG signal is recorded separately and used as the reference input to the LMS filter. In order to avoid these supplementary electrodes a Widrow adaptable structure, was suggested by [24] where the input reference is carried out using band pass filter centered. at the max-

imum energy of ECG signal. This method was not really efficient because the existence of EMG residual in the reference signal, causing the distortion of the original EMG signal. To improve the adaptive filter reference input of [24] we have already suggested an adaptive technique in the precedent studies in which the noise-reference is estimated by a pass-band filter fixed rather on the QRS complex [29]. The obtained results showed a logic amelioration of the EMG/ECG signal to noise ratio.

4.1 The adaptive filtering method

In this section, we have compared the performances by applying two combined adaptive techniques. The two methods for respiratory EMG estimation require an estimation of electrocardiogram interference ECG as a reference signal so that an LMS adaptive filter can be used to cancel ECG in the contaminated EMG signal.

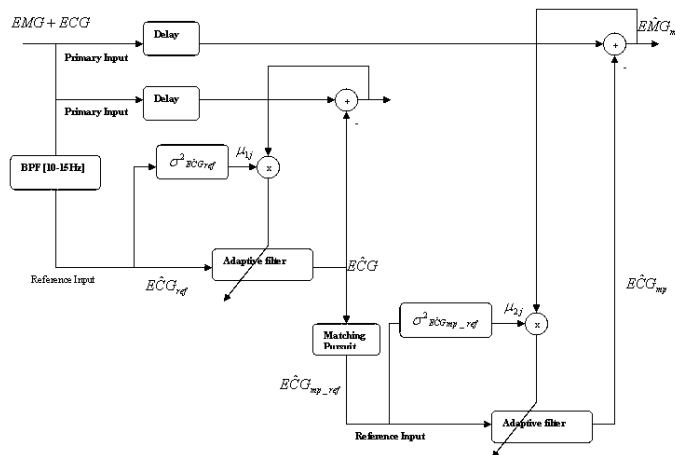


Figure 4.1: The ECG noise canceller algorithm (CAC): $z_j = EMG + ECG$, raw signal; EMG , signal of interest; ECG , noise; \widehat{ECG}_{ref} , reference noise; \widehat{ECG} , estimate of the noise with the adaptive filter; \widehat{H}_j , adaptive filter coefficient; $\widehat{ECG}_{mp.ref}$, estimate of the reference noise with the matching pursuit; \widehat{ECG}_{mp} , estimate of the noise with the adaptive filter; \widehat{EMG}_{mp} , filtered signal at the second step.

The first cascade combined adaptive approach (CAC) proposed for de-noising the respiratory EMG signal (Fig. 4.1) may be divided into two main steps: The first step uses a widrow adaptive filter type LMS and a noise reference extracted by pass-band filtering [10 – 15Hz], this step aims to filter the signal. Whereas to filter the ECG signals again, in order to get a highly qualified input noise reference, the second step applies the matching pursuit algorithm [7, 20, 21]. Then we apply once again the LMS adaptive structure to filter the signal.

The second combined adaptive technique ($BPF_{10-15Hz}$) follows also two steps: the first step applies pass-band filter centered at the QRS complex ($[10 - 15Hz]$), in order to extract the ECG noise reference signal. The second step applies again the same processing shown in the first adaptive technique (CAC).

In this section we use the same LMS algorithm described at section 3.1 except that for the stability of the algorithm, the step-size parameter μ will be restrict according to the following equation

$$\mu_{j+1} = \mu_j + \frac{1}{1 + \sigma_{ECG_{ref_j}}^2}, \quad (4.1)$$

where $\sigma_{ECG_r}^2$ is the power of the reference input.

We choose the Matching Pursuit algorithm for his high resolution and local ability to adapt to transients structures. It is an iterative, non-linear procedure. The MP decomposes signal into the summation of a series of linear expansion function. The waveforms (“atoms”) are selected from a redundant dictionary of vectors of a unit module.

The algorithm of vector pursuit begins by choosing the waveform that matches the signal f , as described in equation (4.3), and at each consecutive steps, the whole dictionary is searched and an atom that is adapted (is largest) to the particular segment of the signal (residuum, left after subtracting results of previous iterations) is picked up.

$$f = \langle f, g_{\lambda_0} \rangle g_{\lambda_0} + R^1 f, \quad (4.2)$$

$$f = \sum_{n=0}^{M-1} \langle R^n f, g_{\lambda_n} \rangle g_{\lambda_n} + R^M f. \quad (4.3)$$

The number of iteration depends on the decomposed signal length; it is fixed after test applied on real situation. The first term $\left(\sum_{n=0}^{M-1} \langle R^n f, g_{\lambda_n} \rangle g_{\lambda_n} \right)$ of equation (9) represent the second step electrocardiogram ECG reference signal estimation $\widehat{ECG}_{mp.ref}$

The algorithm is performed on MatLab using Wave Lab toolbox. For a decomposed signal of $N = 16384$ samples. The number of iteration of the matching pursuit procedure is fixed to 70, to ovoid EMG signal estimation. The FIR filter coefficients are fixed to $32 > 1024/50$.

We select Symmlet wavelet family for their similarity to the ECG signal [5], especially eight order (Symmlet 8) as mother wavelet.

4.2 Results

4.2.1 Performance indicators

However, to quantitatively assess the validity and efficiency of the proposed ECG removal technique we use in this study the most common estimator of amplitude features:

the Average Rectified Value (*ARV*). The average rectified value of signals is defined in percent as

$$ARV_s\% = 100 \frac{\sum_{k=1}^N |s(k)|}{\sum_{k=1}^N |r(k)|}, \quad (4.4)$$

where N represents the number of samples, $s(k)$ the processed signal samples and $r(k)$ the raw respiratory *EMG* signal contaminated with obvious *ECG* artefacts.

To evaluate the effect of the processed methods on the *ECG* and *EMG* signals separately, we use the segments of the *EMG* signal between two consecutive *ECG* spikes ($ARV_{EMG}\%$) free of *ECG* and the segments of consecutive *ECG* spikes ($ARV_{ECG}\%$) free of *EMG* signal [30].

4.2.2 Application to real respiratory *EMG* signal

The adaptive process needs initially an input reference. We present in Figure 4.2 references noise signal estimation of the *ECG* and the processed respiratory *EMG* signal. Raw surface respiratory *EMG* signal contaminated by *ECG* signal is showed in Fig. 4.2a. Fig. 4.2b presents the case of an *ECG* noise reference obtained by the decomposition of the signal with the matching pursuit algorithm (*CAC* method); Fig. 4.2c depicts the case of an *ECG* reference estimated with a pass band filter ($BPF_{10-15Hz}$) fixed on the *ECG-QRS* component [10 – 15Hz]. The Figs. 4.2d and 4.2e show the *EMG* processed signals. When the adaptive filter reference is respectively carried out by the *CAC* method and by applying band-pass filters ([10 – 15Hz]) ($BPF_{10-15Hz}$). It is important to notice the undesirable residual *ECG* signal contained in the *EMG* signal estimation with $BPF_{10-15Hz}$ method as shown in Fig. 4.2e.

According to Table 4.1 it's clear that the best performing reference signal *ECG* extraction is the *CAC* method. However we have a good *ECG* estimation more than 85% without *EMG* residual 0%.

We notice too that the frequency components of the *EMG* signal (less than 20Hz) are better preserved as shown on the Figure 4.3 with *CAC* method. This may be explained by the fact that the LMS filter adapt to *EMG* component that could exist in the reference signal when the $BPF_{10-15Hz}$ method is applied.

In order to better confront the two methods we evaluate separately for each method, the effect of filtering on both *EMG* respiratory signal and *ECG* signal estimation (Table 4.1). The results evaluated show that the $ARV\%$ of *EMG* is more than 99% when we have applied *CAC* method. On the contrary, we loose accounting for the $ARV\%$, more than 10% of signal *EMG* amplitude by applying ($BPF_{10-15Hz}$) method. The two methods applied estimate more than 90% of *ECG* signal amplitude ($ARV\%$), but in reality, *CAC* method has got the highest value which is equal to 98%.

To conclude, it is showed in Figure 4.4 the two phases of surface *EMG* signal filtering.

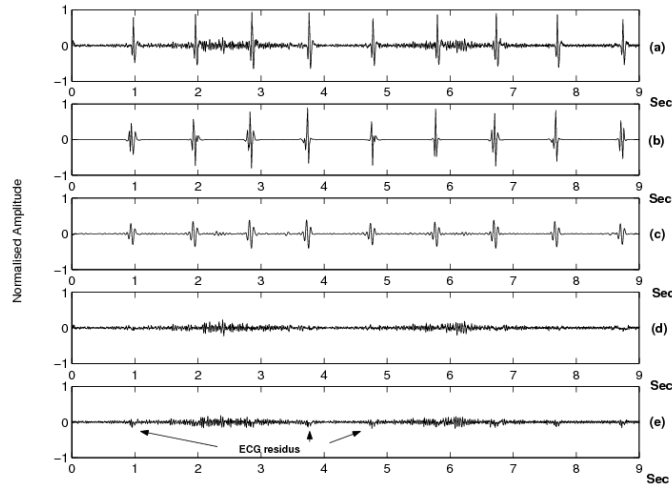


Figure 4.2: Reduction of the *ECG* artifacts:(a) Raw respiratory *EMG* signal contaminated with *ECG* signal.(b): *ECG* noise references signals extracted using matching pursuit (*CAC*) method.(c): *ECG* noise references signals extracted using Band Pass Filter ($BPF_{10-15hz}$) method. (d) Cleaned *EMG* signal with (*CAC*) method. (e) Cleaned *EMG* signal with ($BPF_{10-15hz}$) method.

The first phase consists in filtering (*AIC*) the electromagnetic components 50 Hz and 150 Hz (Fig. 4.4b) then, in the second phase we filter the *ECG* signal by applying the *CAC*

ARV Amplitude in Percent (%)			
Reference signals			
Raw EMG	$EMG_{removal}$ with $BPF_{10-15hz}$	$EMG_{removal}$ with <i>CAC</i>	
100	96	100	
Raw ECG	$ECG_{10-15hz}$ method	ECG_{CAC} method	
100	60	85	
Filtered Signals			
Raw EMG	$EMG_{Distortion}$ with $BPF_{10-15hz}$	$EMG_{Distortion}$ with <i>CAC</i>	
100	10	0.92	
Raw ECG	$ECG_{10-15hz}$	ECG_{CAC}	
100	91	98	

Table 4.1: Average rectified value (ARV) mean of *ECG* and *EMG* components in reference noise signal.and in Filtered Signal using *CAC* and *B.F* methods.

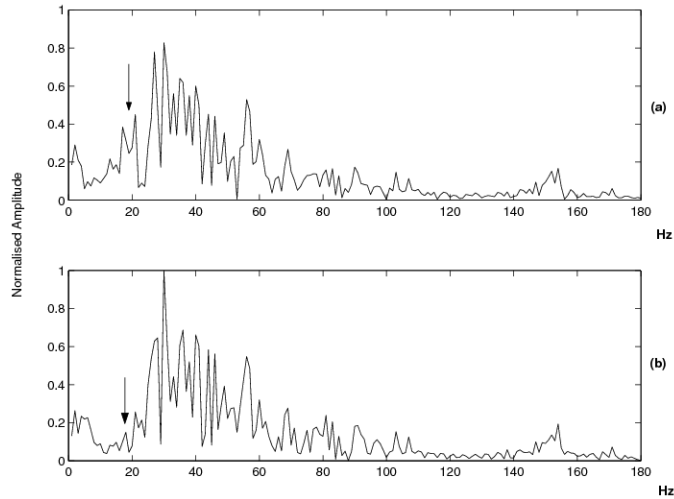


Figure 4.3: Power spectral density estimation of cleaned respiratory *EMG* signal with:(a) *BPF* $10-15\text{Hz}$ method (b) New *CAC* method.

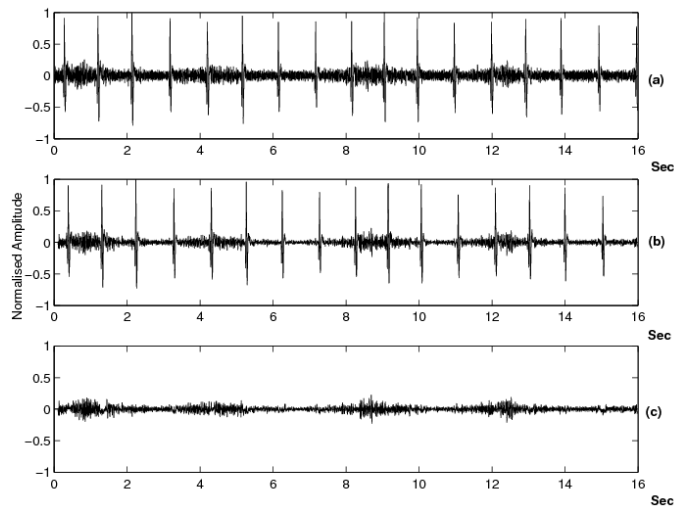


Figure 4.4: Raw surface respiratory *EMG* signal contaminated with *ECG* and power line interference signals; (b) Power line interference removal after applying (*AIC*) algorithm; (c) *ECG* signal removal after applying (*CAC*) algorithm.

method (Fig. 4.4c). The obtained results showed clearly the improvement of the signal to noise *EMG/PLI* and *EMG/ECG* in both cases.

5 Conclusion

In this work we have developed new techniques of noise filtering. In case of electromagnetic interference it is shown that the use of synthesized reference noise with the help of cosines function allows us to get a clean reference noise signal, well correlated with the noise of the primary input. These conditions play an important role in the rate of convergence and rejection bandwidth of the filter. Concerning the cascade adaptive filter of electrocardiogram *ECG* component, it's carried out in two steps. The first one aims at getting the finest *ECG* noise reference signal estimation by combining two structures: an LMS structure in which the reference is performed with a band pass filter $[10 - 15Hz]$ followed by a matching pursuit algorithm. In order to cancel the *ECG* signal the second step applies the LMS structure again with the reference obtained at the first step. This method preserves a large component of *EMG* while effectively eliminating *ECG* artefact. In addition the automatic adjustment of the filter adaptation parameter μ avoids the cumbersome trial and error process needed to choose an adequate value for the step-size parameter. It will increase the speed of convergence of the new structures (*AIC* and *CAC*). and it will also minimize the rejection bandwidth even when the primary input noise increases. Furthermore the proposed procedures may also be applied without the use of supplementary electrode pairs, which will have interesting implications on future usage with fewer cables.

References

- [1] M. Bahoura, M. Hassani, S. G. Lee and M. Hubin, Modification de la méthode de Widrow pour l'élimination de l'interférence 50 Hz du signal ECG, *Innov. Tech. Biol. Med.* **18** (1997), 119–127.
- [2] R. V. Baratta, M. Solomonow, B.-H. Zhou, and M. Zhu, Method to reduce the variability of EMG power spectrum estimates, *Journal of Electromyography and Kinesiology* **8** (1998), 279–285.
- [3] Y. Bensaadoun, K. Raoof, and E. Novakov, Elimination du 50Hz du signal ECG par filtrage adaptatif multidimensionnel, *Innov. Techn. Biol. Med.* **15** (1994), 750–759.
- [4] J. D. Z. Chen, Z. Y. Lin, M. Ramahi, and R. K. Mittal, Adaptive cancellation of ECG artefacts in the diaphragm electromyographic signals obtained through intrasophageal electrodes during swallowing and inspiration, *Neurogastroenterol Mot.* **6** (1994), 279–288.
- [5] V. Cherkassky and S. Kilts, Myopotential denoising of ECG signals using wavelet thresholding methods, *Neural Networks* **14** (2001) 1129–1137.
- [6] I. Christov and I. Dotsinsky, New approach to the digital elimination of 50 Hz interference from electromyogram, *Med Biol Eng Comput.* **26** (1988), 431–434.
- [7] G. Davis, S. Mallat, and Z. Zhang, Adaptive time-frequency decompositions, *Optical Engineering* **33** (1994), 2183–2191.

- [8] Y. Deng, W. Wolf, R. Schnell, and U. Appel, New aspects to event-synchronous cancellation of ECG interference: an application of the method in diaphragmatic EMG signals, *IEEE Trans. Biomed. Eng.* **47** (2000), 1177–1184.
- [9] J. D. M. Drake and J. P. Callaghan, Elimination of electromyogram contamination from electromyogram signals: an evaluation of currently used removal techniques, *Journal of Electromyography and Kinesiology* **16** (2006), 175–187.
- [10] G. S. Furns and W. J. Tompkins, A learning filter for removing noise interference, *IEEE Trans. Biomed. Eng.* **30** (1983), 234–235.
- [11] F. Gideon and A. E. Noujaim, On surface EMG spectral characterization and its application to diagnostic classification, *IEEE Transactions on Biomedical Engineering* **31** (1984), 597–604.
- [12] C. Gondran, E. Siebert, S. Yacoub, and E. Novakov, Noise of surface bio-potential electrodes based on NASICON ceramic and Ag-AgCl, *Med & Biol. Eng & Comput.* **34** (1996), 1–7.
- [13] P. Howells, Intermediate frequency side-lobe canceller, *U.S Patent 3 202 990*, Aug 24, 1965.
- [14] J. C. Huhta and J. G. Webster, 60Hz interference in electrocardiography, *IEEE Trans. Biomed. Eng.* **20** (1973), 91–100.
- [15] M. Kunt, H. Rey, and A. Ligtenberg, Pre-processing of electrocardiograms by digital technics, *Signal Processing* **4** (1982), 215–222.
- [16] S. Levine, J. Gillen, P. Weiser, M. Gillen, and E. Kwatny, Description and validation of an ECG removal procedure for EMGdi power spectrum analysis, *J. Appl. Physiol.* **60** (1986), 1073–1081.
- [17] C. H. Levkov, Fast integer coefficient FIR filter to remove the A.C interference and the high frequency noise component in biological signals, *Med. Biol. Eng. Comput.* **27** (1979), 330–332.
- [18] H. Liang, Z. Lin, and F. Yin, Removal of ECG contamination from diaphragmatic EMG by non linear filtering, *Fourth World Congress of Nonlinear Analysis* **63** (2005), 745–753.
- [19] C. J. De Luca, R. S. Le Fever, and F. B. Stulen, Pasteless electrode for clinical use, *Med. Biol. Eng. Comput.* **17** (1979), 387–390.
- [20] S. Mallat and Z. Zhang, Matching pursuit with time frequency dictionaries, *IEEE Trans. Signal Processing* **41** (1993), 3397–3415.
- [21] S. Mallat, *Une Exploration des Signaux en Ondelette*, Ecole polytechnique, 2000.
- [22] C. Marque, C. Bisch, R. Dantas, S. Elayoubi, V. Brosse, and C. Perot, Adaptive filtering for ECG rejection from surface EMG recordings, *Journal of Electromyography and Kinesiology* **15** (2005), 310–315.
- [23] V. R. Metting, A. Peper, and C. A. Grimbergen, High-quality recordings of bioelectrical events, Part 1: Interference reduction, theory and practice, *Med. Biol. Eng. Comput.* **28** (1990), 389–397.

- [24] K. Raouf, *Traitement du Signal Electromyographique des Muscles Respiratoires et Estimation des Paramètres en Temps réel*, Joseph fourier University of Grenoble France Phd thesis, 1993.
- [25] M. S. Redfern, R. E. Hughes, and D. B. Chaffin, High-Pass filtering to remove electrocardiographic interference from torso EMG recordings, *J. Clin. Biomech.* **8** (1993), 44–48.
- [26] C. Sinderby, L. Lindström, and A. E. Grassino, Automatic assessment of electromyogram quality. Automatic EMG analysis, *Journal of Applied Physiology* **79** (1995), 1803–1815.
- [27] B. Widrow, J. Glover, J. McCool, J. Kaunitz, C. Williams, R. Hearn, J. Zeidler, E. Dong, and R. Goodlin, Adaptive noise cancelling principles and applications, *Proceeding of the IEEE* **63** (1975), 1692–1716.
- [28] B. Widrow, J. M. McCool, M. G. Larimore, and C. R. Johnson, Stationary and non-stationary learning characteristics of the LMS adaptive Filter, *Proceeding of the IEEE* **64** (1976), 1151–1162.
- [29] S. Yacoub, J. Ben Brahim, R. Ketata, P.Y. Gumery, and K. Raouf, Real time Multidimensional treatments of surface electromyographic signals by electrodes array, *Innov. Techn. Biol. Med.* **18** (1997), 267–275.
- [30] P. Zhou and T. A. Kuiken, Eliminating cardiac contamination from myoelectric control signals developed by targeted muscle reinnervation, *Physiological Measurement* **27** (2006), 1311–1327.



Slim Yacoub is an associate professor at the Institut National des Sciences Appliquées et de Technologies de Tunis. He graduated from the Ecole Nationale d'Ingénieur de Tunis and earned his MSc degree from the Institut National Polytechnique de Grenoble France (LEG) and his PhD from the Université Joseph Fourier de Grenoble France (UJFG). His research interests are in signal processing in electromyography.

Kosai RAOOF is an associate professor at the Université Joseph Fourier de Grenoble France. He graduated from the Ecole Nationale d'Ingénieur Université de Bagdad and received his MSc degree from the Institut National Polytechnique de Grenoble France (CEPHAG) and his PhD from the Université Joseph Fourier de Grenoble (UJFG). His research interests are in signal processing in electromyography and in Telecommunication CDMA type.





Hichem Eleuch received electric and electronic engineering diploma from Technical University of Munich in Germany. He obtained his Ph. D. in Quantum Physics from Kastler Brossel Laboratory in Ecole Normale Suprieure de Paris and Universit Pierre-et-Marie-Curie in France. Dr Eleuch is an associate Professor in the National Institute of Applied Science and Technology in Tunisia since 2004. He is an associate member in the International Centre of Theoretical Physics in Trieste Italy since 2006. Currently he is a visiting researcher at the Texas A&M university, College Station Texas, U.S.A. His research interest is related to quantum optics, nonlinear, chaotic and stochastic processes as well as their applications.